Malaysian Journal of Chemistry, 2025, Vol. 27(3), 126-133
(Special Issue: *2nd International Science and Technology Colloquium, i-COSTECH 2024*)

Synthesis, Parameter Optimization and Characterization of $ZnCl_2$ Activated Carbon Derived from Waste Tamarind Seed

Jeyashelly Andas* and Nurlisa Safinaz Naserun
Faculty of Applied Sciences, Universiti Teknologi MARA, Cawangan Perlis, Kampus Arau, Perlis
*Corresponding author (e-mail: drshelly@uitm.edu.my)

A highly surface area activated carbon (AC) was synthesized from waste tamarind seed (TS) using $ZnCl_2$ under different impregnation ratios of raw TS/$ZnCl_2$ (1: 0.5, 1:1, 1:1.5 and 1:2) and activation temperatures ranging 600 to 900 ºC. The resultant AC, char and raw TS were characterized by Fourier transform infrared spectroscopy (FTIR), iodine number (IN), percentage yield (%), CHNS elemental test, proximate analysis, and scanning electron microscope (SEM). The optimum synthesizing condition of (impregnation ratio: 1:1.5 and activation temperature :800 °C) was elected based on the highest IN, registering 905.03 mg/g with a yield % of 24.10. Proximate analysis proved that TS was the best precursor for the production of AC with high volatile (68.24 %) and fixed carbon of 21.90 %. Based on CHNS analysis, a noteworthy rise in Carbon % to 48.52 % was recorded for AC, compared to the raw TS (41.40 %). SEM analysis of AC proved the well-development of porous networks. Disappearance of peaks in the FTIR spectra of AC and char at ~2919 cm^{-1}, 2852 cm^{-1}, 1741 cm^{-1}, 1600-1400 cm^{-1} compared to raw TS signifies the elimination of volatile components during the carbonization and activation process. To conclude, underrated TS was successfully transformed into high value AC.

Keywords: Activated carbon; tamarind seed; $ZnCl_2$; impregnation ratio; fixed carbon

Received: August 2024; Accepted: October 2024

Originated from Madagascar, tamarind (*Tamarindus indica* L.) is often used as fruit jelly, dry fruit or in brews/juice [1]. The two major by-products from tamarind are the pulp and seed [2], in which, tamarind seed (TS) accounts for nearly 34% and often is discarded as a huge waste product after depulping the pod [3]. The conversion of this low cost agro-waste into renowned and sustainable products are grasping the attention of worldwide researchers. For example, in a recent study, tamarind seed polysaccharide was used to synthesize nanoparticles as an oral nanocarrier [4]. In another work, tamarind seed powder was used as a fuel during the preparation of Mn_2O_3 nanoparticles [5].

Since decades, activated carbon (AC) has received an immense global demand arising from its exceptional characteristics such as thermo-stability, high porosity, and surface area [6]. Traditionally, AC is prepared from expensive non-renewable sources such as coal, that is experiencing serious depletion in the coming years. Thanks to the abundantly available biomass that has garnered great exploitation as raw material for AC production. In general, there are two activation steps to prepare AC, namely, physical and chemical activation. Chemical activation in the presence of activators such as $ZnCl_2$, H_3PO_4 and KOH promises countless advantages over physical activation such as increases the percentage yield, reducing the analysis period and lowering the char activation temperature (chemical activation: 400-700°C; physical activation: 700-1100°C) [6]. On top of the list, $ZnCl_2$ appears as one of the most promising activating agents due to its unique characteristics as Lewis acid and strong dehydration effect on lowering the decomposition temperature of lignocellulosic and cellulosic precursors biomass [7]. In addition, $ZnCl_2$ resulted in an improved yield %, compared to 10-40% losses reported over KOH activation [8]. Furthermore, the use of $ZnCl_2$ led to the production of highly surface area and well porous materials, with enhanced oxygen containing group, as reported by Jangra et al. [9] during the synthesis of AC from marigold flower. In a different work by Yağmur and Kaya. [10], $ZnCl_2$ activation of coconut shell had resulted 275 times improved specific surface area of 935.46 m^2/g with an excellent adsorption capacity (156.25 mg/g) of Methylene Blue.

However, to date, there are very scarce work reported on the utilization of TS as a precursor for AC [11-14]. Further, no known studies were reported on the optimization of synthesizing parameters such as impregnation ratio of TS: $ZnCl_2$ and activation temperature. The choice of precursor, activation agent, and process factors is obligatory to obtain high specific surface area AC with enhanced porosity and characteristics, that will determine its performance [15]. Thus, the present work aimed to prepare AC from TS using $ZnCl_2$ as

†Paper presented at the 2nd International Science and Technology Colloquium (i-COSTECH 2024)

the activator under the influence of impregnation ratio and activation temperature and further characterize to provide an insight on the parameter's effect on the textural characteristics of AC.

EXPERIMENTAL

Materials and Methods

Tamarind fruit was purchased from a local market in Langkawi, Malaysia. The chemicals used were zinc chloride ($ZnCl_2$, HmBG), iodine pearl (I_2, HmBG, 99%), sodium thiosulphate-5-hydrate ($Na_2S_2O_3 \cdot 5H_2O$, HmBG, 99%), sodium carbonate anhydrous Na_2CO_3, HmBG 99%), potassium iodate (KIO_3, HmBG, 99.8%), hydrochloric acid (HCl, 37%), potassium iodide (KI, HmBG, 99.87%) and starch ($C_6H_{10}O_5$, HmBG).

Treatment of Tamarind Seed (TS)

Firstly, TS were separated from the pulp and transferred into a container. Later, it was cleaned and rinsed with copious amount of tap water and distilled water, prior to drying at 110°C for 24 h. Then, the dried TS were crushed, grinded and sieved with 200 µm mesh and kept in a closed container for further use.

Synthesis of Activated Carbon (Optimization Studies)

***Effect of impregnation ratio of raw TS:$ZnCl_2$ (mass ratio)*:** The influence of impregnation ratio was examined at 1:0.5, 1:1, 1:1.5 and 1:2 at a constant activation temperature of 800℃ and activation time of 30 min. In brief, to prepare 1:1 (mass ratio), 10 g of TS was soaked with 10 g of $ZnCl_2$ in 20 mL of distilled water, and subsequently stirred (210 rpm) at 110℃ for 2 h for sufficient mixing. Later, the impregnated feedstock was placed in a crucible and oven dried at 110℃ for 5 h prior to activation in the furnace from room temperature to 800℃ with a rate of 20℃/min and an activation time of 30 min. Then, the sample was allowed to cool in desiccator and later, was crushed with pestle and mortar and sequentially washed with 3 M HCl and finally with hot distilled water, until the pH of the washed water attained pH 7. Then, the synthesized material was dried at 110℃ for 5 h and afterwards, was sieved (150 µm), weighed and subjected to yield % measurement using Equation (1) [6] and iodine number (IN) determination according to ASTM D4607-94 [6].

$$\text{Yield (\%)} = \frac{M_F}{M_I} \text{ x } 100\ \% \qquad (1)$$

where M_F = Mass of product; M_I = Mass of precursor

Similar experiments were repeated for all the investigated ratios at constant activation temperature, and likewise, subjected for yield % and IN. The best ratio for the subsequent optimization studies was chosen based on the maximum IN recorded.

***Effect of activation temperature*:** The influence of activation temperature was investigated at a fixed ratio of TS:$ZnCl_2$ and activation time of 30 min, while altering the activation temperature at 600℃, 700℃, 800℃ and 900℃. Similar experimental procedure as described in the preceding section was repeated to obtain the optimal activation temperature.

Material Characterization

The synthesized AC under the optimized condition and raw TS were subjected for CHNS analysis (Thermo Scientific Flash 2000 based on ASTM 3172), SEM (Inspect F50 USA), FTIR (Perkin Elmer Frontier) analysis and proximate analysis (Moisture content (MC), ash content (ASC) and volatile matter (VM) using Equations (2), (3) and (4) [16], respectively. Fixed carbon (FC) was calculated using Eq.(5). For comparison, char was subjected for FTIR and SEM analysis.

$$\text{MC (\%)} = \frac{m_c - m_d}{m_c - m_e} \text{ x } 100\% \qquad (2)$$

where m_c = mass of crucible with sample (g); m_d = mass of crucible with sample after drying (g); m_e = mass of empty crucible (g)

$$\text{ASC (\%)} = \frac{m_c - m_l}{m_c - m_e} \text{ x } 100\% \qquad (3)$$

where m_c = mass of crucible with sample (g); m_l = mass of crucible after weight loss (g); m_e = mass of empty crucible (g)

$$\text{VM (\%)} = \frac{\left[100(m_{ci} - m_{cf}) - \text{MC}(m_{ci} - m_{cl})\right]}{(100 - \text{MC})(m_{ci} - m_{cl}) \text{ x } 100} \qquad (4)$$

where m_{ci} = mass of crucible with sample before heating (g); m_{cf} = mass of crucible with sample after heating (g); m_{cl} = mass of crucible with lid (g); MC = moisture content obtained

$$\text{FC } (\%) = 100\ \% - (\%\ \text{MC} + \%\ \text{VM} + \%\ \text{ASC}) \qquad (5)$$

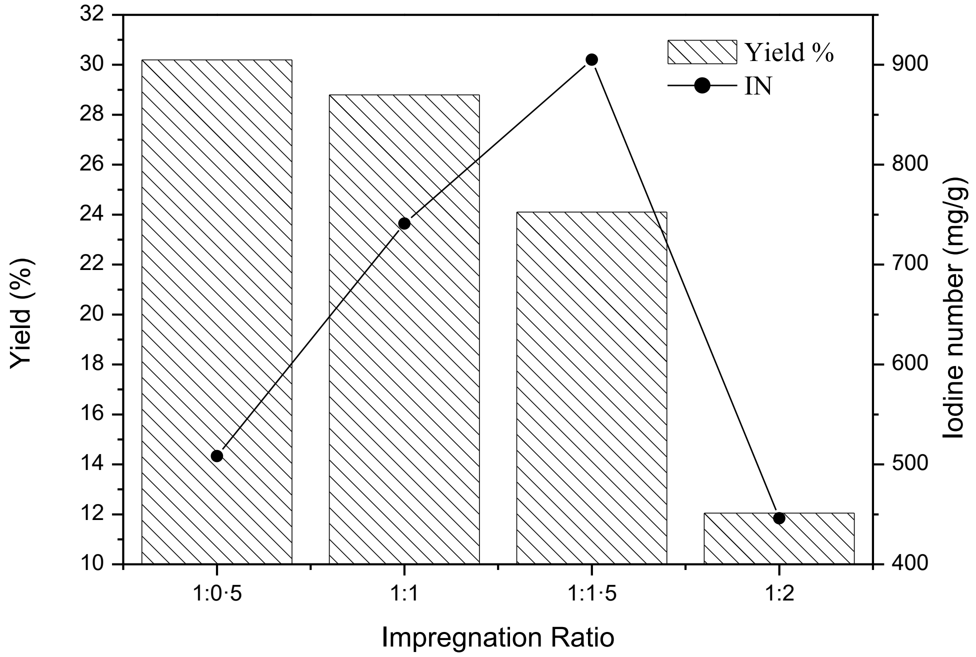

Figure 1. The influence of impregnation ratio on the yield % and IN (mg/g) of the AC.

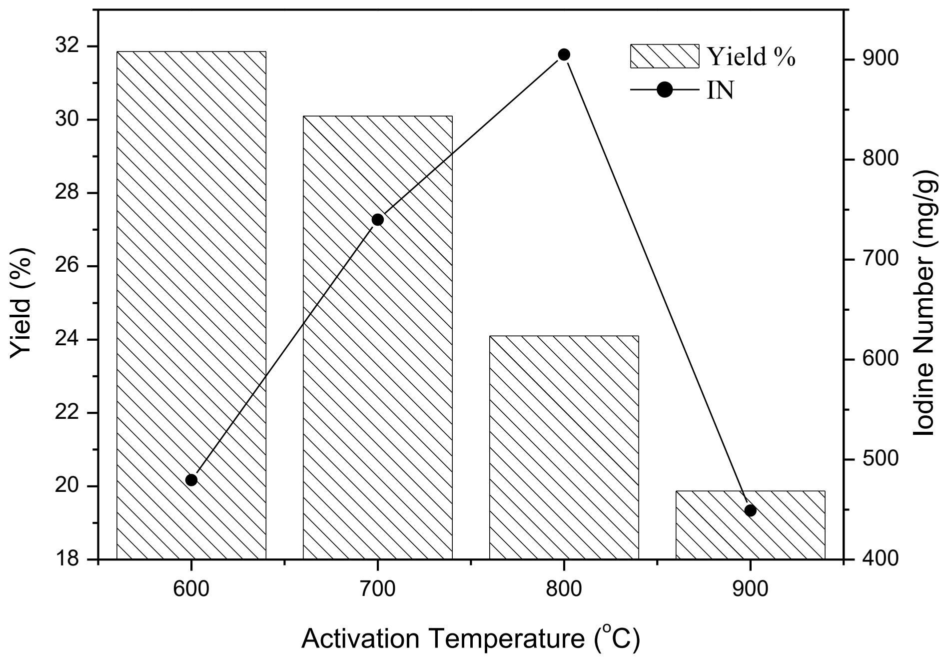

Figure 2. The effect of activation temperature on the yield % and IN (mg/g) of the synthesized AC.

RESULTS AND DISCUSSION

Influence of Impregnation Ratio

IN and yield % reported at different impregnation ratios at constant activation temperature of 800 ℃ are compared in **Figure 1**. Accordingly, a steep decrease in percentage yield from 30.20% to 12.05% was recorded as the impregnation ratio was increased from 1:0.5 to 1:2. During chemical activation of char, high concentration $ZnCl_2$ can accelerate the removal of large quantity of carbon such as CO_2, CH_4 as volatile substance, by rupturing the aliphatic and aromatic bonds, leading to a great decrease in the weight loss, and thereafter reduces the percentage yield of the AC [17]. This is in agreement with Benmahdi et al. [18] whom prepared $ZnCl_2$ activated AC from silver berry seeds. In general, IN reflects the micropore content of AC. IN ranging between 500-1200 mg/g is equivalent to specific surface area of 900-1100 m^2/g [14]. Theoretically, a great IN resembles a high specific surface area AC, that has a significant role in enhancing its adsorption efficiency. In this context, referring **Figure 1**, IN was significantly improved from 1:0.5 (508.26 mg/g) to 1:1.5 (905.03 mg/g). However, 1:2 mass ratio experienced an excessive reduction to 446 mg/g. An increase in micropore content might have caused the rise in IN while excess dehydration and micropores destruction accelerated at a higher impregnation ratio had resulted in lower IN [16]. This phenomenon can also be supported by AC's pore wall thinning, that causes the collapse of pores which inhibits the adsorption of iodine during IN measurement [6]. A similar trend in IN was reported by AC prepared from rice husk [16]. Hence, based on the maximum IN registered, an impregnation ratio of 1:1.5 was selected as the best ratio for the subsequent parameter studies.

Influence of Activation Temperature

The use of $ZnCl_2$ and variation in the activation temperature (600-900℃) at fixed 1:1.5 impregnation ratio and activation time of 30 min, had hugely affected the percentage yield and IN of the AC as displayed in **Figure 2**.

A gradual decrease in percentage yield was observed upon an increase in activation temperature from 600℃ (31.86%) to 700℃ (30.10%). However, a massive drop in yield % was registered with further raising the temperature to 800℃ (24.10%) and 900℃ (19.87%), that signifies, more volatile compounds were released and carbon burn-off was accelerated at higher activation temperature, leading to an immense decrease in the percentage yield. The promotional effect of $ZnCl_2$ and activation temperature was notable on the increasing trend of IN from 479.4 mg/g to 742.0 mg/g and reached maximum, 905.03 mg/g when the temperature rose from 600 to 700 and 800℃, respectively. The steady increment can be attributed to the increase in reaction rate between the $ZnCl_2$ with char, producing more micropores, which is responsible for iodine adsorption. Nevertheless, drastic drop of IN to 449 mg/g at 900 ℃ was due to excess activation of the TS, accelerating the consumption of carbon in TS [19]. In addition, it is suggested due to the rupture of carbon structure, causing the collapsing of smaller pores [6] and reducing the iodine adsorption. Thus, with regard to the highest IN, 800℃ was chosen as the best activation temperature under the studied condition. To conclude, 1:1.5 ratio of raw material: $ZnCl_2$ and 800 ℃ was fixed as the optimal condition.

Ultimate and Proximate Analysis

According to the CHNS analysis, the carbon content in raw TS increased significantly from 41.10% to 48.52% in AC. This proves the successful carbonization and activation process. H content was registered as 6.09% for raw TS and reduced nearly ~92.1% to only 0.48% for AC. This undoubtedly affirms the elimination of volatile compounds during the carbonization. $ZnCl_2$ is known to dissolve cellulose/hemicellulose in biomass and accelerate the removal of hydrogen and oxygen via dehydration [20]. Thus, this proves the effectiveness of $ZnCl_2$ as the activator of TS under the studied parameter condition. Nitrogen content increased slightly from 2.27% for raw TS to 2.75% in AC. Furthermore, no trace amount of sulphur was detected for both raw TS and AC, which suggests the eco-friendly nature of the synthesized AC and TS proved to be a good precursor for the fabrication of AC. **Table 1** summarizes the proximate analysis for the raw TS and the synthesized AC under the optimized condition. Referring **Table 1** moisture content, ash content and fixed carbon were greatly enhanced for AC in comparison to the raw TS. Indonesian Industrial Standard (SII No. 0258-88) has underlined that the moisture content of an AC not greater than 15% is suggested to exhibit good adsorption capacity [21].

Furthermore, the synthesized AC exhibited comparable ash content with commercial powdered activated carbon (WP220) that reported ash content of 10.5% and is also close to steam activated pine nut shell (PNS77, 11.9%) as reported by Mestre et al. [22]. In addition, a huge reduction in the volatile matter for AC agrees well with the removal of volatiles during the activation process that results in the creation of a porous carbonaceous structure that indirectly, leads to higher fixed carbon content. To conclude, raw TS appeared as good precursor as it exhibits low ash content, high volatile content and notable fixed carbon [23].

Table 1. Proximate analysis of raw TS and AC.

Sample	Moisture Content (%)	Ash Content (%)	Volatile Matter (%)	Fixed Carbon (%)
Raw TS	8.0	1.86	68.24	21.90
AC	10.0	11.05	20.05	58.90

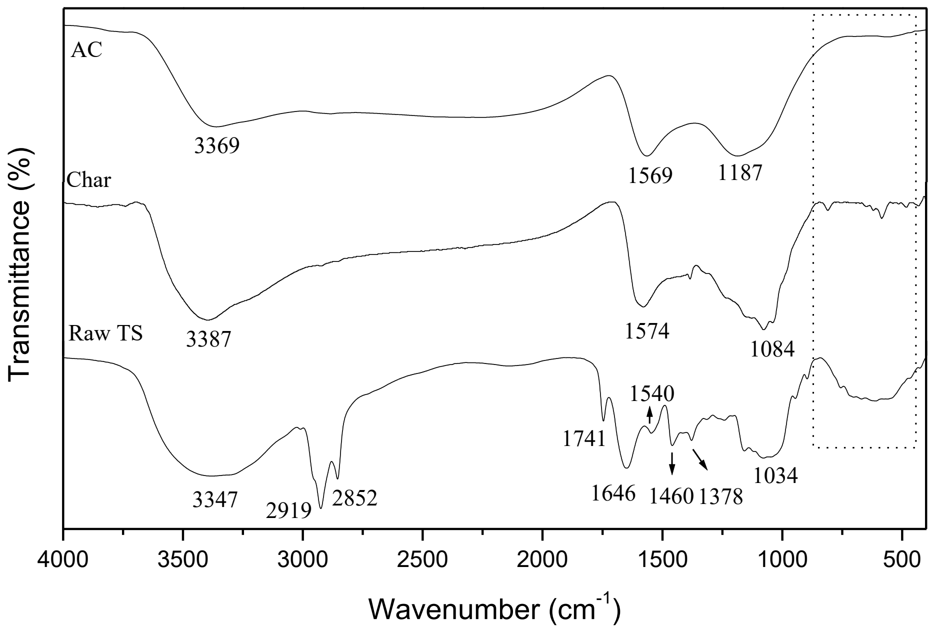

Figure 3. The FTIR spectra of raw TS, Char and AC.

Surface Analysis by FTIR

Figure 3 compares the FTIR spectra of raw TS, char and the synthesized AC. The raw TS apparently showed many adsorption peaks compared to the latter two.

This supports the fact that carbonization route and activation by $ZnCl_2$ had removed most of the volatile matter in char and AC, respectively. In general, all the samples showed broad band at 3347-3387 cm^{-1}, corresponding to the stretching vibration of O-H bond [15]. Nevertheless, the O-H band (3347 cm^{-1}) appeared to be broader for raw TS and experienced red shift towards 3387 cm^{-1} and 3369 cm^{-1} for char and AC, respectively. Strong intense peak at ~1540-1569 cm^{-1} is attributed to stretching vibration of C=C in aromatic ring [24], while C-O stretching vibration of carboxylic acid, alcohol, phenols, esters is evidenced from the existence of peak at ~1034 cm^{-1} [24]. Shifting in the peak was clearly observed for char and AC at ~1084-1187 cm^{-1}. The peaks around 900-600 cm^{-1} are due to C-H vibrations [25]. To note, several adsorption peaks are present only for raw TS. For example: i) ~2925 cm^{-1} and 2855 cm^{-1} (C-H asymmetric aliphatic hydrocarbon [15]), ii) 1741 cm^{-1} (C=O stretching of ester band of cellulose)[26] ,iii) 1600-1400 cm^{-1} (stretching vibration of C=O, C=C and bending vibration of N-H) [19]. To conclude, successful carbonization and $ZnCl_2$ activation process was evidenced through the disappearance and shifting of several peaks in the IR spectra of char and AC.

Morphological Analysis by SEM

Figure 4 displays the SEM micrographs of the prepared samples at x1000 magnification. Referring **Figure 4(a)**, globular like surface was exhibited by raw TS with no porosity development. This was undoubtedly caused by the absence of any activation process. On contrary, formation of pores was observed at certain regions of the char surface (**Figure 4(b)**). Upon $ZnCl_2$ activation, porosity with wide opening was greatly enhanced for AC as shown in **Figure 4(c)**, resulting from the release of water and organic compounds [12] during the activation stage. A similar SEM observation for carbonized $ZnCl_2$ AC was captured by Ishak and Kumar [12]. To sum up, $ZnCl_2$ activation had resulted in the formation of porous AC that was indisputably affected by the synthesis parameters.

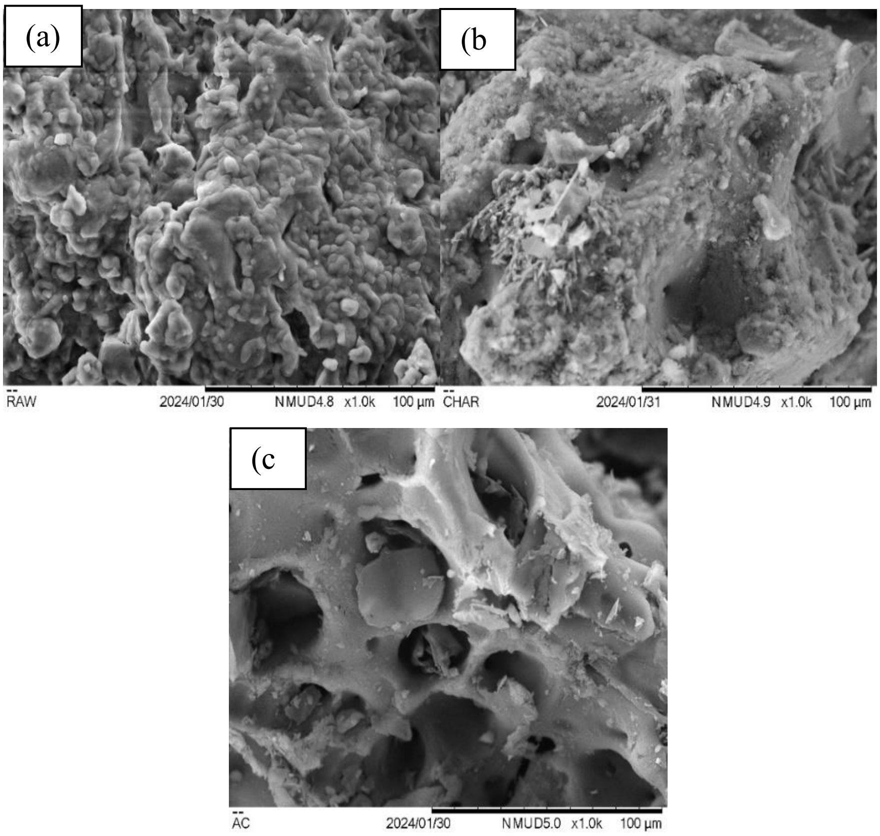

Figure 4. SEM images of (a) raw TS; (b) char and (c) AC.

CONCLUSION

A green approach for the conversion of waste TS into AC, comparable to reported literatures was successfully done under the influence of different impregnation ratio and activation temperatures. Activation temperature (600-900 ℃) and impregnation ratios (1:0.5-1:2) resulted in the production of AC with IN ranging from 406 to 905.3 mg/g, with yield % varying from 12.05%-31.06%. Under the optimized process parameters, maximum IN of 905 mg/g with 24.10% yield was recorded for the AC, suggesting the capability of TS as the precursor. Loss of several IR peaks and porosity development through SEM investigation clearly demonstrate the impact of synthesizing parameters on the formation of AC. To conclude, this facile activation had successfully transformed an underutilized agro-waste into a green material under the influence of different synthesizing parameters that undoubtedly play a significant role in enhancing the AC's properties.

ACKNOWLEDGEMENT

J. Andas thanks Universiti Teknologi MARA for providing the instrumentation assistance throughout the completion of the project.

REFERENCES

1. Martins, C. M., Guedes, J. A. C., de Brito, E. S. and Ferreira, S. R. S. (2022) Valorization of tamarind seeds using high-pressure extraction methods to obtain rich fractions in fatty acid and phenolic compounds. *The Journal of Supercritical Fluids*, **183**, 105556.

2. Okello, J., Okullo, J. B., Eilu, G., Nyeko, P. and Obua, J. (2017) Mineral composition of Tamarindus indica LINN (Tamarind) pulp and seeds from different agro-ecological zones of Uganda. *Food Science & Nutrition*, **5**(5), 959–966.

3. Mansingh, B. B., Binoj, J. S., Sai, N. P., Hassan, S. A., Siengchin, S., Sanjay, M. R. and Liu, Y. C. (2021) Sustainable development in utilization of Tamarindus indica L. and its by-products in industries: A review. *Current Research in Green and Sustainable Chemistry*, **4**, 100207.

4. Javaid, A., Singh, A., Parvez, S., Negi, M. and Mudavath, S. L. (2024) Carboxymethyl Tamarind seed polysaccharide nanoparticles as a potent mucomimetic and biocompatible oral nanocarrier. *Colloids and Surfaces A: Physicochemical and Engineering Aspects*, **682**, 132889.

5. Premakumari, P., Latha, H. K. E. and Nagaraju, G. (2022) Green synthesis of dimanganese trioxide nanoparticles using tamarind seed powder: effect of tamarind seed powder concentration on the structural, electrical and electrochemical properties of dimanganese trioxide nanoparticles. *Materials Today: Proceedings*, **49**, 554–558.

6. Andas, J., Rahman, M. L. A. and Yahya, M. S. M. (2017) Preparation and characterization of activated carbon from palm kernel shell. In *IOP Conference Series: Materials Science and Engineering*, *IOP Publishing*, **226**, 1, 0121562017, August 2017.

7. Farma, R., Julita, R. I., Apriyani, I., Awitdrus, A. and Taer, E. (2023) $ZnCl_2$-assisted synthesis of coffee bean bagasse-based activated carbon as a stable material for high-performance supercapacitors. *Materials Today: Proceedings*, **87**, 25–31.

8. Pimentel, C. H., Díaz-Fernández, L., Gómez-Díaz, D., Freire, M. S. and González-Álvarez, J. (2023) Separation of CO_2 using biochar and KOH and $ZnCl_2$ activated carbons derived from pine sawdust. *Journal of Environmental Chemical Engineering*, **11(6)**, 111378.

9. Jangra, R., Mahendia, P., Karakoti, M., Sahoo, N. G., Srivastava, A., Sinha, O. P., Clemons, T. D., Deshpande, U. and Mahendia, S. (2024) $ZnCl_2$-assisted conversion of nitrogen-containing biomass carbon from marigold flower: Toward highly porous activated nitrogen-doped carbon for low ESR and enhanced energy density supercapacitors. *Journal of Energy Storage*, **75**, 109728.

10. Yağmur, H. K. and Kaya, İ. (2021) Synthesis and characterization of magnetic $ZnCl_2$-activated carbon produced from coconut shell for the adsorption of methylene blue. *Journal of Molecular Structure*, **1232**, 130071.

11. Sharada, S., Sri, N. B., Supriya, K., Venkatesh, M. and Srihari, M. (2016) Adsorption of toxicants (chromium, iron and oxalic acid) on activated carbons prepared from tamarind seeds. *International Journal for Scientific Research and Development*, **1(5)**, 274–283.

12. Ishak, Z. and Kumar, D. (2022) Adsorption of methylene blue and reactive black 5 by activated carbon derived from tamarind seeds. *Tropical Aquatic and Soil Pollution*, **2(1)**, 1–12.

13. Andas, J. and Satar, N. A. A. (2018) Synthesis and characterization of tamarind seed activated carbon using different types of activating agents: a comparison study. *Materials Today: Proceedings*, **5(9)**, 17611–17617.

14. Mopoung, S., Moonsri, P., Palas, W. and Khumpai, S. (2015) Characterization and properties of activated carbon prepared from tamarind seeds by KOH activation for Fe (III) adsorption from aqueous solution. *The Scientific World Journal*, **2015(1)**, 415961.

15. Jawad, A. H., Abd Malek, N. N., Khadiran, T., ALOthman, Z. A. and Yaseen, Z. M. (2022) Mesoporous high-surface-area activated carbon from biomass waste via microwave-assisted-H_3PO_4 activation for methylene blue dye adsorption: An optimized process. *Diamond and Related Materials*, **128**, 109288.

16. Njewa, J. B., Vunain, E. and Biswick, T. (2022) Synthesis and Characterization of Activated Carbons Prepared from Agro-Wastes by Chemical Activation. *Journal of Chemistry*, **2022(1)**, 9975444.

17. Hock, P. E., and Zaini, M. A. A. (2018) Activated carbons by zinc chloride activation for dye removal–a commentary. *Acta Chimica Slovaca*, **11(2)**, 99–106.

18. Benmahdi, F., Oulmi, K., Khettaf, S., Kolli, M., Merdrignac-Conanec, O. and Mandin, P. (2021) Synthesis and characterization of microporous granular activated carbon from Silver berry seeds using $ZnCl_2$ activation. *Fullerenes, Nanotubes and Carbon Nanostructures*, **29(9)**, 657–669.

19. Lan, X., Jiang, X., Song, Y., Jing, X. and Xing, X. (2019) The effect of activation temperature on structure and properties of blue coke-based activated carbon by CO_2 activation. *Green Processing and Synthesis*, **8(1)**, 837–845.

20. Li, B., Li, C., Li, D., Zhang, L., Zhang, S., Cui, Z., Wang, D., Tang, Y. & Hu, X. (2023) Activation of pine needles with zinc chloride: Evolution of functionalities and structures of activated carbon versus increasing temperature. *Fuel Processing Technology*, **252**, 107987.

21. Zulkania, A., Hanum, G. F. and Rezki, A. S. (2018) The potential of activated carbon derived from bio-char waste of bio-oil pyrolysis as adsorbent. In *MATEC Web of Conferences*, *EDP Sciences*, **154**, 01029.

22. Mestre, A. S., Viegas, R. M., Mesquita, E., Rosa, M. J. and Carvalho, A. P. (2022) Engineered pine nut shell derived activated carbons for improved removal of recalcitrant pharmaceuticals in urban wastewater treatment. *Journal of Hazardous Materials*, **437**, 129319.

23. Naji, S. Z. and Tye, C. T. (2022) A review of the synthesis of activated carbon for biodiesel production: Precursor, preparation,

and modification. *Energy Conversion and Management: X*, **13**, 100152.

24. Andas, J. and Wazil, N. (2019) From waste mango kernel into high surface area activated carbon. *Materials Today: Proceedings*, **19**, 1541–1546.

25. Raut, E. R., Bedmohata, M. A. and Chaudhari, A. R. (2022) Comparative study of preparation and characterization of activated carbon obtained from sugarcane bagasse and rice husk by using H_3PO_4 and $ZnCl_2$. *Materials Today: Proceedings*, **66**, 1875–1884.

26. Andas, J. and Idris, N. N. (2021) Green synthesis of mesoporous carbon from kapok. In *AIP Conference Proceedings, AIP Publishing*, **2332**, 1, February, 2021.